ELSEVIER

www.elsevier.nl/locate/carres

Carbohydrate Research 325 (2000) 177–182

CARBOHYDRATE RESEARCH

The conformation of α-(1→4)-linked glucose oligomers from maltose to maltoheptaose and short-chain amylose in solution

Hiroshi Sugiyama [a,*], Toyohiko Nitta [b], Maki Horii [b], Kyoko Motohashi [b], Jun Sakai [b], Taichi Usui [c], Kanehiko Hisamichi [d], Jun-ichi Ishiyama [e]

[a] *Institute for Chemical Reaction Science, Tohoku University, Sendai 980, Japan*
[b] *Biomedical Laboratory, Kureha Chemical Industry Co. Ltd., Tokyo 160, Japan*
[c] *Department of Applied Biochemistry, Shizuoka University, Shizuoka 422, Japan*
[d] *Tohoku College of Pharmacy, Sendai 983, Japan*
[e] *Fukushima National College of Technology, Iwaki 970, Japan*

Received 18 February 1998; accepted 5 November 1999

Abstract

The conformation of maltose-type oligomers in water and in dimethylsulfoxide (Me_2SO) was studied using two-dimensional NMR spectra. In Me_2SO all of the oligomers have a **1a**-type conformation. In water, they tend to adopt the same conformation, but the oligomers are looser and more flexible than in Me_2SO.

Keywords: Amylose; Maltose; Oligomer; Conformation; NMR

1. Introduction

Amylose, with an α-(1→4)-linked glucose unit, forms the backbone chain in starch. Many basic textbooks describe its conformation as a helical coil having a **1a**-type conformation and not a **1b** type [1]. However, these conformational studies are based on X-ray diffraction of its glycerol complex [2], its viscosity [3], and the well-known classical amylose–iodine color reaction. We do not consider that these studies provide direct evidence for a helical coil conformation in solution. Therefore, we examined the conformation of maltose-type oligomers in solution using two-dimensional NMR spectra.

2. Methods

NMR methods.—The small oligomers from maltose to maltoheptaose were kindly donated by Nippon Shokuhin Kako Co., Ltd., and the short-chain amylose (mean molecular weight 2900) was purchased from Nakarai Kagaku Co., Ltd. The spectra of these oligomers were recorded without further purification.

^2H_2O (D_2O) and [$^2H_6$]dimethylsulfoxide (Me_2SO) were selected as solvents. These are the NMR solvents normally used for oligosaccharides and provide different environments for the solute. The NMR spectra were recorded using Jeol Lambda 600 spectrometers at 600 MHz for protons and at 150 MHz for carbon. Sodium 4,4-dimethyl-4-sila-[$^2H_4$]pentanoate was used as the internal stan-

* Corresponding author. Fax: +81-22-2238956.

0008-6215/00/$ - see front matter
PII: S0008-6215(99)00310-9

dard in both solvents. In the Me_2SO solutions, a few drops of D_2O were added to eliminate hydroxyl-proton coupling. For the phase-sensitive, rotatory frame nuclear Overhauser effect (ROESY) spectra of the oligomers, mixing times between 10 and 300 ms were used; the observed frequency offset was at least 600 Hz lower than the lowest anomeric proton signal, and the waiting time between scans was 3.2 s [4–7]. Carbon–proton three-bond coupling constants were measured using the 2D version method of Wilker and Leibfritz [8]. The τ_{max} was 200 ms with six or eight samplings of τ between 40 and 180 ms, and the gradient ratios used were $G_1:G_2:G_3 = 2:2:1$. The Karplus-type equation relating carbon–proton three-bond coupling constants and dihedral angles used in this paper is that derived experimentally by Mulloy et al. [9].

The proton spectra of all of the oligomers were assigned using phase-sensitive double-quantum-filtered correlation spectra, and we confirmed the existing assignments using proton–carbon heteronuclear correlation spectra [4,10].

Estimation of diatomic distances.—Diatomic distances were estimated using the program CAChe (CAChe Scientific, Inc., UK).

3. Results and discussion

Assignments of the proton spectra in D_2O are given in Table 1. The chemical shifts and vicinal proton–proton coupling constants of the ring protons of the reducing-end residues, the internal residues, and the non-reducing-

Table 1
Proton chemical shifts (ppm) and coupling constants (Hz) of maltose-type oligomers in D_2O [a]

Position	1	2	3	4	5	6	6′
Maltose							
α	5.23	3.57	3.98	3.65	3.72	3.76	3.90
	(J_{12} 3.67)	(J_{23} 9.15)	(J_{34} 9.05)	(J_{45} 9.16)	(J_{56} 6.2, $J_{56'}$1.6)	($J_{66'}$ −12.3)	
β	4.66	3.28	3.78	3.67	3.60	3.84	3.95
	(J_{12} 8.06)	(J_{23} 8.06)	(J_{34} 8.45)	(J_{45} 8.43)			
N	5.42	3.59	3.75	3.42	3.71	3.76	3.90
	(J_{12} 3.66)	(J_{23} 9.89)	(J_{34} 9.16)	(J_{45} 9.34)	(J_{56} 6.2, $J_{56'}$ 1.6)	($J_{66'}$ −12.3)	
Maltotriose							
α	5.23	3.57	3.98	3.66	3.79	3.83	3.87
	(J_{12} 3.97)	(J_{23} 10.38)	(J_{34} 9.31)	(J_{45} 9.77)			
β	4.66	3.28	3.78	3.66	3.60	3.78	3.91
	(J_{12} 8.08)	(J_{23} 9.16)	(J_{34} 10.07)	(J_{45} 9.77)	($J_{56'}$ 1.98)	($J_{66'}$ −12.05)	
m	5.41	3.66	3.98	3.66	3.79	3.83	3.87
	(J_{12} 3.66)	(J_{23} 11.9)	(J_{34} 9.31)	(J_{45} 9.77)			
n	5.40	3.59	3.74	3.43	3.69	3.83	3.87
	(J_{12} 3.66)	(J_{23} 10.07)	(J_{34} 9.61)	(J_{45} 9.61)			
Maltoheptaose							
α	5.23	3.57	3.97	3.67	3.83	3.83	3.85
	(J_{12} 4.02)	(J_{23} 9.72)	(J_{34} 9.35)	(J_{45} 8.98)			
β	4.65	3.27	3.77	3.69	3.59	3.83	3.90
	(J_{12} 8.06)	(J_{23} 8.06)	(J_{34} 9.52)	(J_{45} 9.52)			
m	5.41	3.63	3.96	3.66	3.83	3.83	3.85
	(J_{12} 4.03)	(J_{23} 9.16)	(J_{34} 9.16)	(J_{45} 9.16)			
n	5.40	3.59	3.70	3.42	3.75	3.83	3.85
	(J_{12} 3.67)	(J_{23} 8.98)	(J_{34} 9.53)	(J_{45} 9.53)			
Short-chain amylose							
m	5.41	3.64	3.97	3.67	3.85	3.83	3.87
	(J_{12} 3.98)	(J_{23} 9.99)	(J_{34} 9.28)	(J_{45} 8.99)			

[a] α, α anomer of the reducing-end residue; β, β anomer of the reducing-end residue; m, internal (middle) residue; n, non-reducing-end residue.

Table 2
Proton chemical shifts (ppm) and coupling constants (Hz) of maltose-type oligomers in Me_2SO [a]

Position		1	2	3	4	5	6	6′
Maltose								
α		5.01 (J_{12} 3.66)	3.32 (J_{23} 10.24)	3.76 (J_{34} 8.40)	3.39 (J_{45} 9.31)	3.72	3.69	3.69
β		4.40 (J_{12} 7.63)	3.05 (J_{23} 8.39)	3.49 (J_{34} 9.31)	3.38 (J_{45} 9.16)	3.30 (J_{56} 5.80)	3.61 ($J_{66'}$ −12.36)	3.76
n	α	5.08 (J_{12} 3.35)	3.33 (J_{23} 9.46)	3.46 (J_{34} 9.16)	3.16 (J_{45} 9.16)	3.56 (J_{56} 5.80)	3.54 ($J_{66'}$ −11.29)	3.68
	β	5.10 (J_{12} 3.36)						
Maltotriose								
α		5.02 (J_{12} 3.66)	3.32 (J_{23} 9.92)	3.78 (J_{34} 9.36)	3.43 (J_{45} 8.45)	3.67	3.67	3.73
β		4.42 (J_{12} 7.94)	3.07 (J_{23} 8.24)	3.52 (J_{34} 9.15)	3.40 (J_{45} 9.42)	3.34	3.61	3.71
m	α	5.09 (J_{12} 3.97)	3.42 (J_{23} 9.92)	3.74 (J_{34} 9.36)	3.43 (J_{45} 8.45)	3.67	3.67	3.73
	β	5.11 (J_{12} 3.02)						
n		5.12 (J_{12} 3.67)	3.36 (J_{23} 9.92)	3.48 (J_{34} 9.30)	3.18 (J_{45} 9.30)	3.58	3.67	3.70
Maltoheptaose								
α		4.99 (J_{12} 3.46)	3.27 (J_{23} 10.00)	3.77 (J_{34} 9.31)	3.39 (J_{45} 9.33)	3.64	3.64	3.69
β		4.40 (J_{12} 7.63)	3.04 (J_{23} 9.17)	3.48 (J_{34} 9.16)	3.37 (J_{45} 7.64)	3.58	3.58	3.73
m	α	5.07 (J_{12} 3.66)	3.39	3.70	3.40	3.64	3.64	3.73
	β	5.09						
m	5.09							
n		5.09 (J_{12} 3.36)	3.32 (J_{23} 10.07)	3.45 (J_{34} 9.16)	3.14 (J_{45} 9.16)	3.55	3.53	3.68
Short-chain amylose								
m		5.10 (J_{12} 3.45) −5.17	3.41	3.73	3.44	3.65	3.65	3.71

[a] Symbols as in Table 1.

end residues of the oligomers are almost the same in D_2O. In consequence, in this paper, only the proton assignments for maltose, maltotriose, maltoheptaose, and short-chain amylose are shown with the glucose ring conformation in the $^4C_1$ form.

However, in Me_2SO, the overlap resulting from slightly different chemical shifts and the broader peaks of the internal residues of the oligomers made it difficult to determine the spin–spin coupling constants. However, the vicinal coupling constants of the ring protons of maltotriose in Me_2SO showed that the units in maltotriose have a typical $^4C_1$ conformation. Furthermore, the chemical shifts of maltotriose and the other oligomers were almost identical. Therefore, even in Me_2SO, the maltose-type oligomers should have the $^4C_1$ ring conformation (Table 2).

When we tried to measure the nuclear Overhauser effect spectra (NOESY) for the oligomers, the only well-resolved spectrum we obtained was for short-chain amylose, because of the correlation between the observed frequency and the correlation time of the samples studied [4–7]. Therefore, the ROESY

spectra of all of the oligomers were measured and satisfactory results were obtained. Recently, Wilker and Leibfritz reported a very convenient method for measuring carbon–proton long-range couplings [8]. Their method for estimating the dihedral angles of the inter-residual linkages was used for the carbon–proton three-bond couplings of the oligomers. First we examined the present combined method [8,9] in comparison with X-ray crystallographic data of cyclomalto-hexa-, -hepta-, and -octaoses [11], since these small cyclodextrins can be expected to have the same conformation in both the crystal and in solution. The differences between these results were within 0.1 Hz in the inter-residue $^3J_{C-H}$ constants.

In Me_2SO, all of the NOE spectra of the oligomers shorter than the octaose showed cross-peaks between the anomeric protons of the non-reducing-end residues and H-4 of the contiguous residues, with mixing times ≤ 30 ms [6], and between these peaks and the peaks between the anomeric protons of the non-reducing-end residues and H-2 of the same residues, with a mixing time of 300 ms. The intensities of the cross-peaks between the non-reducing-end residues and H-3 and H-5 of the contiguous ones were almost zero when compared with the cross-peaks mentioned above, even with a mixing time of 300 ms, while no cross-peak was observed between the anomeric proton and H-6*s* and H-6*r*.

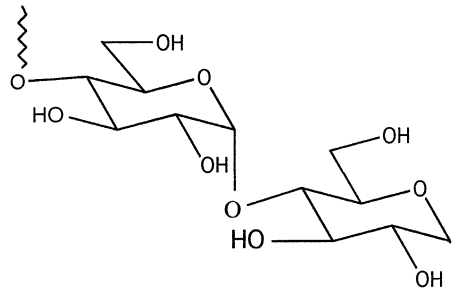

1a

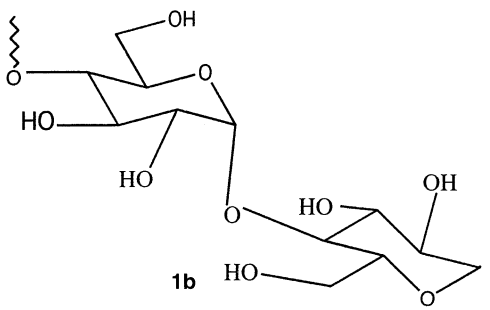

1b

These facts suggest that the non-reducing-end residues are very close to H-4 of the contiguous residues, as shown in Structure **1a**. As shown in Table 3, the carbon–proton three-bond coupling constants of the inter-residual bonds of the oligomers in Me_2SO had similar values. The experimentally derived Karplus-type equation, reported by Mulloy et al. [9], gave almost identical values for H-1′–C-1′–O–C-4 (ϕ) and C-1′–O–C-4–H-4 (φ). These results suggest that there are four possible combinations of dihedral angles for ϕ and φ, namely $++$, $+-$, $-+$, and $--$. Based

Table 3
$^3J_{C-H}$ coupling constants and dihedral angles of the linkage bonds between the residues [a]

	In D_2O		In Me_2SO	
	$^3J_{H1-C4}$ (Hz) ϕ	$^3J_{H4-C1}$ (Hz) φ	$^3J_{H1-C4}$ (Hz) ϕ	$^3J_{H4-C1}$ (Hz) φ
Maltose	3.53 − 54.5°	1.01 70.5°	4.28 − 28°	5.41 0°
Maltotriose	4.68 ± 22°	4.37 ± 27°	4.48 − 25°	5.28 −9°
Maltotetraose	4.04 ± 31°	4.58 ± 23.5°	4.43 − 26°	5.00 − 16°
Maltopentaose	4.19 ± 29°	4.70 ± 21.5°	4.46 − 25.5°	5.33 − 6.5°
Maltohexaose	3.72 − 34°	4.47 − 25°	4.68 − 22°	5.19 − 11.5°
Maltoheptaose	3.89 − 33°	4.75 − 21°	4.57 − 23.5°	5.00 − 16°
Short-chain amylose	3.38 − 38°	5.17 − 12°	4.57 − 23.5°	5.12 − 13.5°

[a] The Karplus-type equation used in this Table is $^3J_{C-H} = 5.5\cos^2\theta - 0.7\cos\theta + 0.6$ [9].

on the crystallographic study of amylose, which has been shown to be a left-handed helical coil [2], the dihedral angles in Me_2SO were selected between 0 (5.41 Hz) and $-16°$ (5.00 Hz) for φ, and between -22 (4.68 Hz) and $-33°$ (4.28 Hz) for ϕ. From estimation by the program CAChe, the distances between the anomeric protons of the non-reducing-end residues and H-4 of the contiguous ones were determined to be 0.2064–0.1964 nm, distances which violate the van der Waals radius of hydrogen. The distance between H-1 and H-2 in the same residues was 0.246 nm, which is almost equal to the van der Waals radius. These distances are useful for interpreting our NOE spectra. They provide evidence that in Me_2SO the oligomers should have the classic helical coil conformation or a very similar one.

The ROESY spectrum for maltose in D_2O was different from that in Me_2SO. It showed a cross-peak between the anomeric proton of the non-reducing-end residue and H-4 of the reducing-end residue and a cross-peak between the anomeric proton and H-2 in the same residue with a mixing time of 30 ms. These peaks had almost the same intensity. The **1a**-type conformer should be dominant. The spectrum of maltotriose showed strong cross-peaks between the anomeric protons of the non-reducing-end residues and H-4 of the contiguous residues. Weak cross-peaks appeared between the anomeric protons and H-2 in the same residues. At mixing times of 30 and 300 ms maltotetraose, -pentaose, -hexaose, -heptaose, and short-chain amylose all showed cross-peaks between the anomeric protons of the non-reducing-end residues and H-4 of the contiguous residues, and weak cross-peaks between the anomeric protons and H-2 in the same residues.

As with Me_2SO, the inter-residue carbon–proton three-bond coupling constants of the oligomers studied were measured, and are shown in Table 3. The coupling constants for maltose were very different from those of the other oligomers. The dihedral angles determined from these coupling constants were $\phi = 54.5°$ and $\varphi = 70°$. If the $+,+$ or $-,-$ pairs of dihedral angles are selected, the diatomic distance between the anomeric proton of the non-reducing-end residue and H-4 of the reducing-end residue is 0.3097 nm. This value is much greater than that between the anomeric proton and H-2 in the same residue (0.246 nm). On this basis, the $+,-$ or $-,+$ pairs of dihedral angles should be selected. In these cases, the corresponding diatomic distance was 0.2502 nm, a value close to the distance between the anomeric proton and H-2 in the same residue. On this basis, its NOE spectrum can be rationalized. The crystallographic study of methyl β-maltoside monohydrate, which shows $\phi = -9.1°$ and $\varphi = 9.1°$, was taken into consideration [12], and the pair $\phi = -54.5°$ and $\varphi = 70°$ was selected. This ϕ coupling constant is the same coupling as measured (3.5 Hz) for maltose by Pérez et al. in water [13]. However, in D_2O the triose, tetraose, and pentaose have slightly different ϕ angles from the longer oligomers. For any pair of signs of the dihedral angles, the atomic distances (0.1948–0.2194 nm) between H-1 of the non-reducing-end residues and H-4 of the contiguous residues can be rationalized. This leads to the conclusion that these three oligomers have conformations intermediate between those of maltose and amylose. In the oligomers longer than the pentamer, the pair of $+,-$ or $-,+$ dihedral angles results in an overlap of both end residues similar to that seen in the cyclodextrins, which have a pair of $-,+$ dihedral angles [11]. Again, based on the crystallographic study of amylose [2], the pair of $-,-$ dihedral angles was selected.

There are many theoretical studies on the conformation of maltose, the maltooligomers, and amylose [14]. However, to our knowledge, there is no study that takes our results into consideration, particularly in the case of maltose. Hricovini et al. have made similar interpretations in their NMR and theoretical studies of methyl β-xylobioside in various solvents [15]. Their work shows that precise solvent contribution should taken into account in theoretical calculations.

The mean residue number of the short-chain amylose is 16 or 17, and it has almost three complete turns of the helical coil. Nevertheless, its ϕ and φ angles in both solvents, Me_2SO and D_2O, were not appropriate angles for the formation of hydrogen bonding be-

tween O-3 and O-2′ of the contiguous residues. Methyl β-maltoside in the crystal state shows ϕ and φ angles suitable for formation of O-3 and O-2′ hydrogen bonds [16]. This is one of the factors lowering the conformational energy, and the crystallographic analysis of maltohexaose complexed with glycogen phosphorylase showed similar ϕ and φ angles (see Fig. 4 in Ref. [16]).

The ϕ and φ angles of maltose in D_2O were much more open than those of methyl β-maltoside monohydrate in the crystal state, while those in Me_2SO had a pair of different signs and were much more open than those of α-maltose in the crystalline state [12]. The ϕ and φ angles of the short-chain amylose studied were also much more open than the dihedral angles compatible with hydrogen bonding between O-3 and O-2′. Therefore, the energy-lowering factors for amylose in both solvents might result from side-by-side interaction of adjacent glucose residues in the same helical coil. The internal side-by-side interaction of amylose in water might be relatively weak. In Me_2SO, amylose might have a much stronger side-by-side type of energy-lowering factor than in water. A water molecule is much smaller than a molecule of Me_2SO. Since water can act as both a hydrogen-bond donor and acceptor, and the ϕ and φ angles of amylose in water are more open than in Me_2SO, then perhaps water molecules are situated between glucose residues in the amylose helical coil and act to weaken this side-by-side interaction of the coils.

References

[1] (a) R.C. Bohinski, *Modern Concepts of Biochemistry*, second ed., Worth, New York, 1979, p. 264. (b) D. Voet, J.G. Voet, *Biochemistry*, Wiley, New York, 1990, p. 256. (c) J.D. Rawn, *Biochemistry*, N. Paterson, Burlington, NC, 1989, p. 387. (d) E.E. Conn, P.K. Stampf, G. Bruening, R.H. Doi, *Outlines of Biochemistry*, fifth ed., Wiley, New York, 1987, p. 48.

[2] S.D.H. Hulleman, W. Helbert, H. Chanzy, *Int. J. Biol. Macromol.*, 18 (1996) 115–122.

[3] (a) Y. Nakata, S. Kitamura, K. Takeo, T. Norisuye, *Polym. J.*, 26 (1994) 1085–1085. (b) T. Norisue, *Polym. J.*, 26 (1994) 1303–1307. (c) T. Norisue, *Food Hydrocoll.*, 10 (1996) 109–115.

[4] (a) R.R. Ernst, G. Bodenhausen, A. Wokaun, *Principles of Nuclear Magnetic Resonance in One and Two Dimensions*, Clarendon Press, Oxford, 1987. (b) G.E. Martin, A.S. Zektzer, *Two-Dimensional NMR Methods for Establishing Molecular Connectivity*, VCH, New York, 1988.

[5] A.A. Bothner-By, R.I. Stephens, J. Lee, C.D. Warren, R.W. Jeanloz, *J. Am. Chem. Soc.*, 106 (1984) 811–813.

[6] (a) A. Kalk, H.J.C. Berendesen, *J. Magn. Reson.*, 24 (1976) 343–366. (b) S.L. Gordon, K. Wuetrich, *J. Am. Chem. Soc.*, 100 (1978) 7094–7096. (c) R. Boelens, G.W. Vuister, T.M.G. Koning, R. Kaptein, *J. Am. Chem. Soc.*, 111 (1989) 8525–8526. (d) J.N. Breg, R. Boelens, G.W. Vuister, R. Kaptein, *J. Magn. Reson.*, 87 (1990) 646–651.

[7] D. Neuhause, M. Williamson, *The Nuclear Overhauser Effect in Structural and Conformational Analysis*, VCH, New York, 1989, pp. 312–329.

[8] W. Wilker, D. Leibfritz, *Magn. Reson. Chem.*, 33 (1995) 632–638.

[9] B. Mulloy, T.A. Frenkiel, D.B. Davies, *Carbohydr. Res.*, 184 (1988) 39–46.

[10] T. Usui, N. Yamaoka, K. Matsuda, K. Tuzimura, H. Sugiyama, S. Seto, *J. Chem. Soc., Perkin Trans 1*, (1973) 2425–2432.

[11] K. Harata, *Trends Phys. Chem.*, 1 (1991) 45–60.

[12] (a) S.S.C. Chu, G.A. Jeffrey, *Acta Crystallogr.*, 23 (1967) 1038–1049. (b) G.A. Quigley, A. Sarko, R.H. Marchessault, *J. Am. Chem. Soc.*, 92 (1970) 5834–5839.

[13] S. Pérez, F. Taravel, C. Vergelati, *Nouv. J. Chim.*, 9 (1985) 561–564.

[14] A.D. French, J.W. Brady (Eds.), Computer Modeling of Carbohydrate Molecules, ACS Symp. Series 430, Am. Chem. Soc., Washington, DC, 1990. (b) C. Fringant, I. Tvaroska, K. Mazeau, M. Rinaudo, J. Desbrieres, *Carbohydr. Res.*, 278 (1995) 27–41. (c) K.-H. Ott, B. Meyer, *Carbohydr. Res.*, 281 (1996) 11–34.

[15] M. Hricovini, I. Tvaroška, J. Hirsch, *Carbohydr. Res.*, 198 (1990) 193–203.

[16] F. Goldsmith, S. Sprang, R. Fletterick, *J. Mol. Biol.*, 156 (1982) 411–427.